ACS APPLIED MATERIALS & INTERFACES

Research Article

www.acsami.org

High-Performance, Single-Layer Antireflective Optical Coatings Comprising Mesoporous Silica Nanoparticles

Jonathan Moghal,*[,†] Johannes Kobler,[§] Jürgen Sauer,[§] James Best,[‡] Martin Gardener,[‡] Andrew A.R. Watt,[†] and Gareth Wakefield[‡]

[†]Department of Materials, University of Oxford, Parks Road, OX1 3PH Oxford, United Kingdom

[‡]Oxford Advanced Surfaces Group plc, Begbroke Science Park, Oxford OX5 1PF, United Kingdom

[§]NanoScape AG, Am Klopferspitz 19, 82152 Planegg-Martinsried, Germany

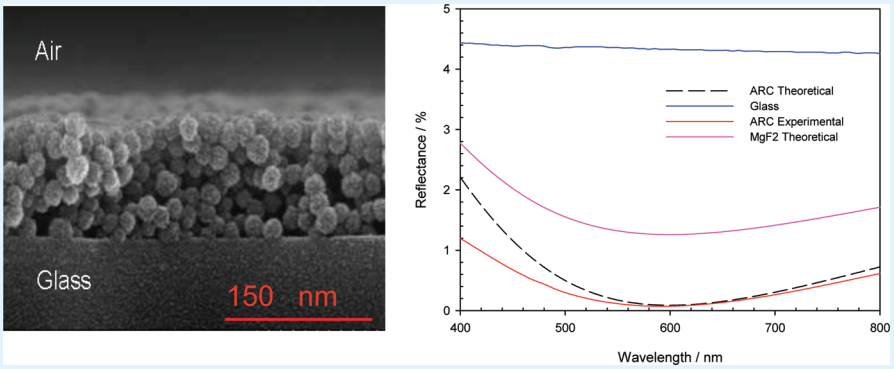

ABSTRACT: Mesoporous silica nanoparticles are used to fabricate antireflectance coatings on glass substrates. The combination of mesoporous silica nanoparticles in conjunction with a suitable binder material allows mechanically robust single layer coatings with a reflectance <0.1% to be produced by simple wet processing techniques. Further advantages of these films is that their structure results in broadband antireflective properties with a reflection minimum that can tuned between 400 nm and 1900 nm. The ratio of binder material to mesoporous nanoparticles allows control of the refractive index. In this report, we discuss how control of the structural properties of the coatings allows optimization of the optical properties.

KEYWORDS: *Antireflection, mesoporous silica, nanoparticles, refractive index*

INTRODUCTION

Antireflection coatings (ARCs) are widely used to increase transmission and reduce the glare resulting from window coatings in a diverse range of industries such as photovoltaics, buildings, displays, and ophthalmic lenses.[1−10] However, current costs per square meter limit take up in cost sensitive industries such as photovoltaics, and consequently the development of low-cost ARCs is an active area of scientific research.

Reflection from any given interface at normal incidence is related to the ratio of the refractive indices of the materials forming the interface and is given by

$$R = \left(\frac{(n_0 - n_m)^2}{(n_0 + n_m)^2}\right) \Big/ 100 \quad (1)$$

where R is % reflectance, n_0 is the refractive index of the first layer (usually air), and n_m is the refractive index of the second layer (window).[10,11]

For example, a crown glass window in air with $n_0 = 1$ and $n_m = 1.52$ gives a reflectance at normal incidence of 4.3% per surface (i.e., a total reflectance of 8.6% from the window). To minimize or remove this reflectance completely, we coated a further layer of refractive index, n_1, on to the window such that the reflections from the air/coating and coating/window interfaces undergo destructive interference to the greatest possible extent. In this general case, the reflectance is given by

$$R = \left(\frac{n_1^2(n_0 - n_m)^2\cos^2 k_0h + (n_0n_m - n_1^2)^2\sin^2 k_0h}{n_1^2(n_0 + n_m)^2\cos^2 k_0h + (n_0n_m + n_1^2)^2\sin^2 k_0h}\right) \Big/ 100 \quad (2)$$

Where k_0 is the phase angle of the incoming light and h is the optical thickness of the film. Under the condition $K_oh = \pi/2$,[10,11] which is equivalent to saying the film thickness $d = \lambda_0/(4n_1)$ at incident wavelength λ_0, eq 2 becomes

$$R = \left(\frac{(n_0n_m - n_1^2)^2}{(n_0n_m + n_1^2)^2}\right) \Big/ 100 \quad (3)$$

Received: November 2, 2011
Accepted: December 21, 2011
Published: December 21, 2011

Therefore, the reflection equals zero when $n_1 = (n_0 n_m)^{1/2}$.[10,11]

For normal incident light of wavelength 550 nm (green light), a perfect antireflective coating on a crown glass window will have a thickness of 112 nm and a refractive index of 1.23. As the angle of incidence increases, the reflection from a surface cannot be defined using eqs 1 and 2. The effects of an incoming electromagnetic wave striking an interface between two different dielectric media are then described using Fresnel's equations. These equations relate the reflected and transmitted field amplitudes to the incident amplitude by way of angles of incidence θ_i and transmission θ_t. For linear light having an $\vec{E}$ field parallel to the plane of incidence, the amplitude reflection coefficient can be defined as parallel reflection ($R_\parallel$), the ratio of the reflected to incident electric field amplitudes. When the electric field is normal to the incident plane, we get perpendicular reflection ($R_\perp$).[10,11] The reflectance of $R_\parallel$ and $R_\perp$ is therefore described by eqs 4 and 5.

$$R_\parallel = \left(\frac{\tan^2(\theta_i - \theta_t)}{\tan^2(\theta_i + \theta_t)}\right) \Big/ 100 \tag{4}$$

$$R_\perp = \left(\frac{\sin^2(\theta_i - \theta_t)}{\sin^2(\theta_i + \theta_t)}\right) \Big/ 100 \tag{5}$$

These equations show that as the angle of incidence increases, the reflectance also increases, which is a function of the refractive index of the material in question. It is desirable to have a low refractive index material for optimum antireflection properties on typical window materials. For the purpose of ARCs, we are interested only in $R_\perp$, as it can never be zero, whereas $R_\parallel$ is zero when the denometer is infinite[10,11]

Current ARC technology relies primarily upon vacuum deposition techniques such as sputtering or physical and chemical vapor deposition.[12,13] High-quality vacuum deposited coatings are expensive and also suffer from fundamental material limitations. The current principal component of antireflection technology is thin films of magnesium fluoride (MgF_2) which has a refractive index of 1.38; the lowest for any solid material.[14] A MgF_2 thin film with thickness of 137.5 nm will result in a reflection minimum of 1.32% at 550 nm. Although MgF_2 is probably the most widely used thin film material for ARC, its performance is not exceptional in single layer form. In order to further improve performance the construction of complex multilayer coatings is generally require.[15−17]Silicon dioxide and titanium dioxide are commonly used materials for these structures as an alternative or in conjunction with fluoride layers.[18−20] Zero reflectance cannot be achieved with a single layer coating due to the absence of suitable low refractive index materials. One solution to this is to fabricate a multilayer system. A thin layer of materials with a high refractive index is placed next to the substrate so as to make it appear to have a higher index; hence an MgF_2 layer is more effective. A two-layer ARC will provide a lower reflectance at a given wavelength but has a narrower bandwidth. For higher performances, further layers are required. Three and four layer coatings have been designed and zero reflectance has been achieved; however, this requires vacuum processing as precise control of film thickness and stack structure is essential.[21,22]

There are alternative approaches to vacuum deposited multilayer stacks.[18−20] Ideally, it is desirable to move away from multilayer stacks and have a single-layer ARC from a cost and processing perspective. A number of examples have been discussed in the scientific literature,[3,23−28] and these approaches can be divided into two categories. The first and most common approach is a sol−gel route, in which chemical precursors (inorganic salts or metal alkoxides) are mixed with water and catalyst to cause hydrolysis and polycondensation.[3,25,29−33] However, reported reflection properties are not equal to multilayer coatings; for example, recent literature quotes a minimum reflection ∼0.8%.[25] There is also typically a high temperature sintering (200−500 °C) step involved to densify the pores of the sol−gel limiting the coatings applicability to glass substrates only.[3,26]

Nanoparticle systems based on materials such as SiO_2 can also be used to create single layer antireflection (SLAR) coatings.[33−35] The reflection of these nanoparticle SLAR coatings can reach as low as 0.5%;[35] however, these films are typically produced by self-assembly methods, such as electrostatic attraction between charged colloidal particles.[33] This results in a high surface roughness which impairs their resistance to mechanical abrasion[36] and limits practical applicability.[33−35] The use of hollow silica nanoparticles has been shown to reduce the refractive index of antireflection coatings further although no binder system is used in these coatings, rather the refractive index is tuned by variation in the core to shell thickness ratio.[37,38] Calcination of nanoparticle coatings has been demonstrated to improve mechanical properties, although this approach does limit the choice of substrates.[39]

To move away from vacuum deposition multi layer ARCs, it is necessary to present a low-cost, low-reflection SLAR coating that can withstand mechanical stress and can be applied to various substrates using simple wet deposition techniques at ambient temperatures.

In this paper, we describe the deposition of mesoporous silica nanoparticles in a silica binder on glass substrates and show how the coating microstructure relates to the optical properties. Mesoporous is defined by the IUPAC as having a pore size of 2−50, in the case of the particles under discussion the pore size is 2−4 nm.[40] The ARC is deposited using wet deposition techniques, such as spin or dip coating, as it allows accurate control of film thickness. There is no temperature curing process involved; hence the coatings are potentially applicable to various polymer substrates. When using a binder system in conjunction with the mesoporous particles it is possible to fine-tune the refractive index to match the substrate material to achieve optimum antireflection properties on any given window material. A layer of the mesoporous silica particles has a refractive index of 1.12, and addition of the binder material increases the refractive index to the optimum value calculated by eq 3. With variations of nanoparticle/binder ratio it is possible to tune the refractive index of the coating to obtain <0.1% reflectance, exceeding the properties available for any other single layer ARC system. With this combination of binder and porous nanoparticles a single layer ARC has been developed with a minimum reflectance in the visible of <0.1%. Complete control of the refractive and thickness allows the reflection minimum can be tailored for specific applications.

EXPERIMENTAL SECTION

Mesoporous silica nanoparticles (5.6 wt %) were supplied by NanoScape AG, (Germany). The particles are dispersed and suspended in an anhydrous methanol solution. The nanoparticle/methanol solution was diluted down to 1.5%wt. The binder solution is

made up of 100 μL of tetraethyl orthosilicate (TEOS), 2 mL of isopropanol and 50 μL of 0.1 M hydrochloric acid (HCL). The antireflective coatings were prepared on 10 × 10 cm glass purchased from Soham Scientific. The substrates were cleaned with isopropanol and air-dried before a Chemat Technology KW-4A spin coater was used to deposit the particles. The silica nanoparticles and the binder are mixed together in an appropriate ratio. The change in refractive index is a function of how much binder is inserted into the gaps between the silica particles. By varying the concentration, spin speed and dwell time, the thickness of the film can be altered to give a minimum reflection (maximum transmission) at a desired wavelength.

High resolution scanning electron microscopy (SEM) images were taken using a JEOL 6400 field emission Scanning Electron Microscope operated at 5KV. Bright field transmission electron micrographs (TEM) of nanoparticle samples were taken using a 400 keV high-resolution JEOL 4000HR transmission electron microscope. Particles were dispersed onto holey carbon grids supplied by Agar Scientific.

Transmission and reflectance spectra were recorded using a Perkin-Elmer Lambda 950 UV/vis spectrometer. The reflectance spectra were recorded using the Universal Reflectance Accessory (URA) supplied by Perkin-Elmer. The refractive index was measured using a Horiba Auto SE ellipsometer. For ellipsometry measurements films were deposited on silicon substrates using the same deposition procedure as for glass substrates.

Atomic force microscopy was performed using a digital instruments D3000 large sample AFM with a micro fabricated Si cantilever tip. The measurement was performed in "tapping mode" in air. White light interferometry was performed using a Veeco optical profiler.

Nanoindentation was performed using a Micro Materials NanoTest, Indentations of 0.05mN were performed at room temperature with a Berkovich indenter with 30s hold period at peak load. Five indentations were performed on each film coating.

RESULTS AND DISCUSSION

As previously discussed the addition of the TEOS binder serves two functions. First it was used to increase the refractive index of the ARC to the desired value. Figure 1 shows a plot of the minimum reflection achieved as a function of binder to particle ratio. The mesoporous silica particles spun down on glass can achieve a minimum reflection of 0.28%. Upon addition of the TEOS, this reflection can be reduced to 0.07%. There is a limitation to the amount of binder that can be added. The maximum loading ratio that can be achieved without loss of the optical properties is 30−45%v/v. From Figure 1, it can be seen that even at a loading of 52.8%v/v the optical properties can be deemed acceptable; however, above this loading ratio, the optical properties are compromised. The second function of the TEOS binder is to improve the mechanical properties of the ARC. Good mechanical properties of the ARC are essential for potential commercial applications. The hardness values for the individual loadings of TEOS binder are also plotted in Figure 1. The figure demonstrates that as the loading ratio of binder is increased the hardness of the coating increases; however, above 45% v/v binder loading, the reflectance will begin to increase. The minimum reflection occurs with a 35%v/v loading of TEOS binder which produces a hardness of 4.4 GPa. This value is comparable to various other nanoparticle protective coatings.[41−43] A more common and simple approach used for mechanical testing is a pencil hardness test. A hardness value of 4.4 GPa will pass a 5H pencil test, which is above the industry standard of 3H required for practical applications.[44] Initial data shows that the films will pass a steel wool test (1 kg weight over 10 passes) with minimal scratching visible and no film delamination.[45,46] Consequently, a loading ratio of 35% v/v TEOS binder was chosen as the optimum ratio for the fabrication of the ARC in this study.

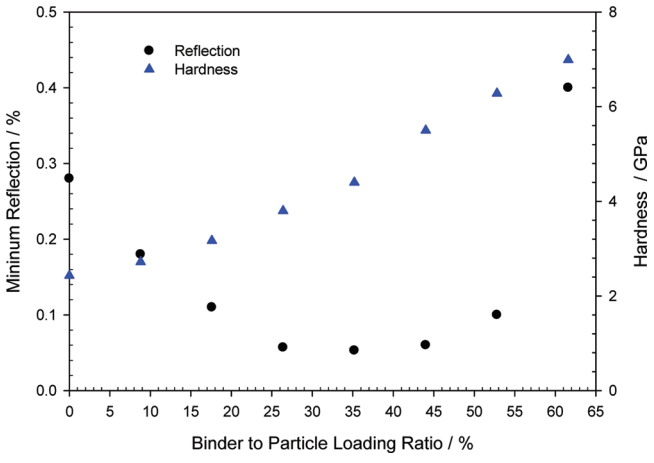

Figure 1. Reflection and hardness as a function of binder to particle loading ration.

A high-resolution bright-field TEM image of the nanoparticles is shown in Figure 2a, with the image is defocused to highlight the pore structure. The nanoparticles have a size distribution from 20 to 30 nm. The pore size is of the particles is approximately 3 nm. It is the ratio of pore to particle volume which controls the refractive index of the particles − this should be as high as possible to allow the maximum loading of a binder system to be introduced between the particles to match the refractive index to the substrate and give maximum mechanical strength to the layer.

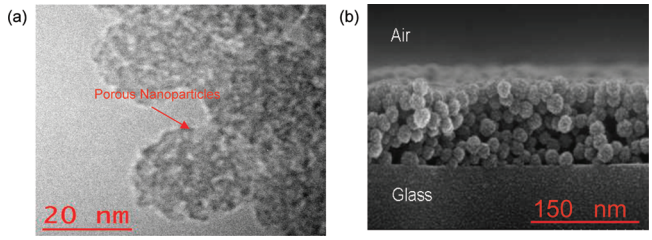

Figure 2. (a) High-resolution TEM images of mesoporous silica nanoparticles. The particles were deposited on a holey carbon grid. (b) Cross-section SEM image of nanoparticle antireflective coating.

Figure 2b shows a high-resolution cross-sectional SEM image of an ARC film on a glass substrate. The SEM cross-section image shows that the nanoparticles are densely packed and that the film thickness is uniform. Although the image contrast is primarily derived from the nanoparticles rather than the binder system it is clear that the film is a single-layer system and the binder is therefore distributed between the nanoparticles and acting as structural reinforcement in addition to modulating the refractive index. It is assumed TEOS molecules have migrated into the spaces between the silica nanoparticles.

An average thickness of 120 ± 5 nm can be obtained from the cross-section image. Film roughness, R_a, has been measured by white light interferometry at 10 nm (Figure 3a). The AFM topography image is shown in Figure 3b. It shows that that the ARC has a nonporous surface profile with roughness on the scale of the particle size with binder filling in the gaps between the particles.

Figure 4 shows the mapping ellipsometry results for the ARC on a silicon substrate. A film of mesoporous silica nanoparticles

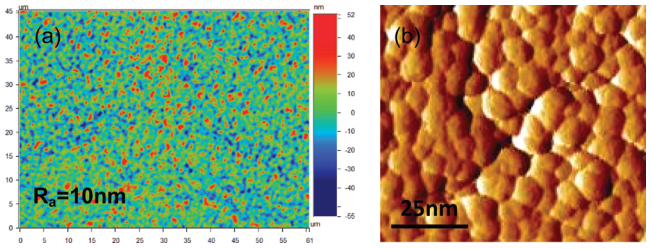

Figure 3. (a) White light interferometry surfaces profile of film. (b) AFM topography image of antireflective coating.

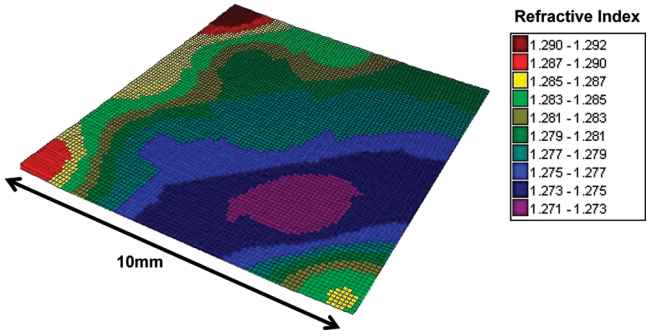

Figure 4. Mapping ellipsometry of ARC on a silicon substrate with a minimum of 590 nm.

without binder has a refractive index of 1.12 ± 0.01. This is significantly lower than common low refractive index materials such as MgF_2 (1.38) and other mesoporous silica particles reported throughout the literature.[47] A refractive index value of 1.1.2 is lower than the optimum refractive index for zero reflectance. Incorporation of the binder increases the coating refractive index to 1.28 ± 0.01. The variation of refractive index over the coating area is negligible and therefore we can conclude the particles and binder form a uniform film across the substrate. Calculations using an effective medium approximation and a silica refractive index of 1.52 suggest that the mesoporous silica nanoparticles have a porosity of approximately 71%. Nitrogen absorption experiments give a particle surface area of 588 ± 4 m^2 g^{-1}.

Figure 5a shows the reflectance for a glass side and an ARC at near normal (8°) incidence. The glass slide has a reflection of 4.4% between 590 and 600 nm, whereas the ARC has a reflection minimum of 0.07%@590 nm (cf. MgF_2 minimum of 1.32%@590 nm). Figure 5a shows that the ARC has a relatively broadband response throughout the visible spectrum (400−800 nm). A plot of eq 2 for this ARC is also given in Figure 5a. The experimental and theoretical curves show significant divergence below 500 nm, with the nanoparticle ARC having a broader antireflection response than that expected from the calculated curve. Such effects are commonly associated with Rayleigh scattering of nanoparticle composite thin films − Rayleigh scattering is strongly dependent on wavelength (λ^4) and hence any effects are most noticeable in the blue part of the spectrum.[10,11] Also shown is the calculated reflectance spectrum for MgF_2 (same film thickness as ARC). This is shown as a comparison between a typical vacuum deposited single-layer ARC and the mesoporous silica ARC reported in this work.

Using the mesoporous silica nanoparticles with a combination of silica binder it is possible to reduce the reflection down to almost zero for normal incidence light. Figure 5(b) shows the effects on the reflection coefficient of the ARC with increasing incident angle along with the calculated values from eqs 4 and 5. At 65°, the glass has a reflectance of 25%, whereas the ARC has a significantly reduced reflectance of 11%.

Applications such as solar and optical windows may require an ARC with minimum reflection shifted to the infrared part of the solar spectrum. By changing the concentration and spin coating conditions the reflectance minimum (at normal incidence) may be shifted with no loss of performance up to 1900 nm. Figure 6a shows the effect of the thickness variations on the coatings. A film thickness of 380 nm is required to provide a reflection minimum at 1900 nm. A cross section SEM of the coatings is shown in Figure 2b. The packing, film roughness and uniformity are the same as the film in Figure 2b. The only parameter that has changed is the film thickness. The precise control of thickness and of the refractive index of the coating makes it a highly flexible system and therefore attractive for multiple window applications.

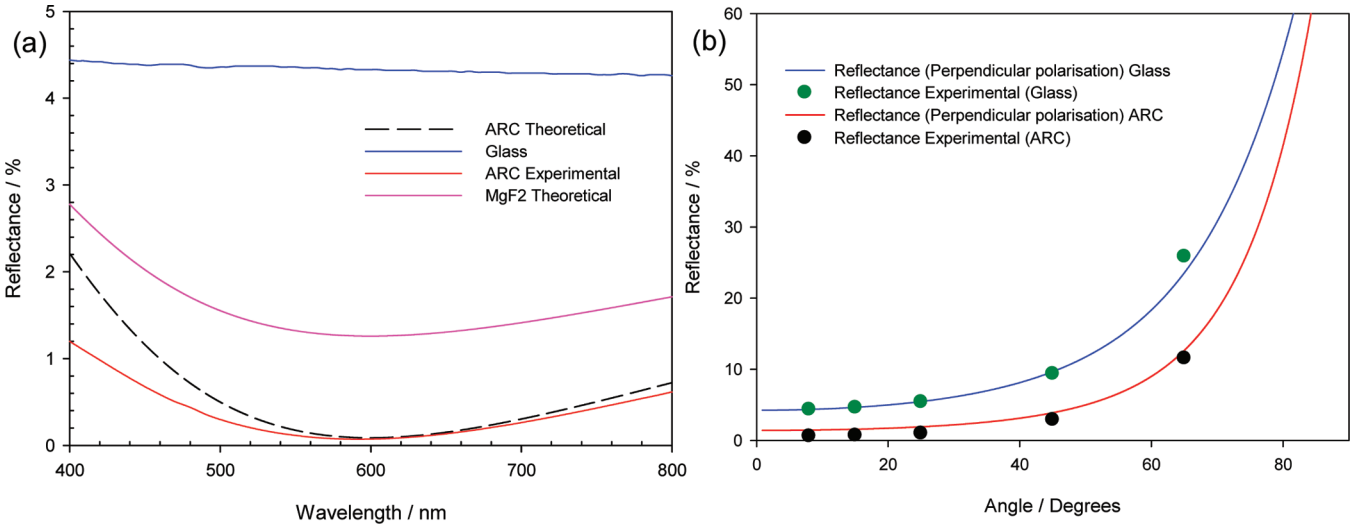

Figure 5. (a) Experimental reflection spectra of glass and ARC and theoretically calculated reflection spectra for ARC and MgF2. (b) Reflection versus incident angle experimental and theoretically calculated for ARC and glass.

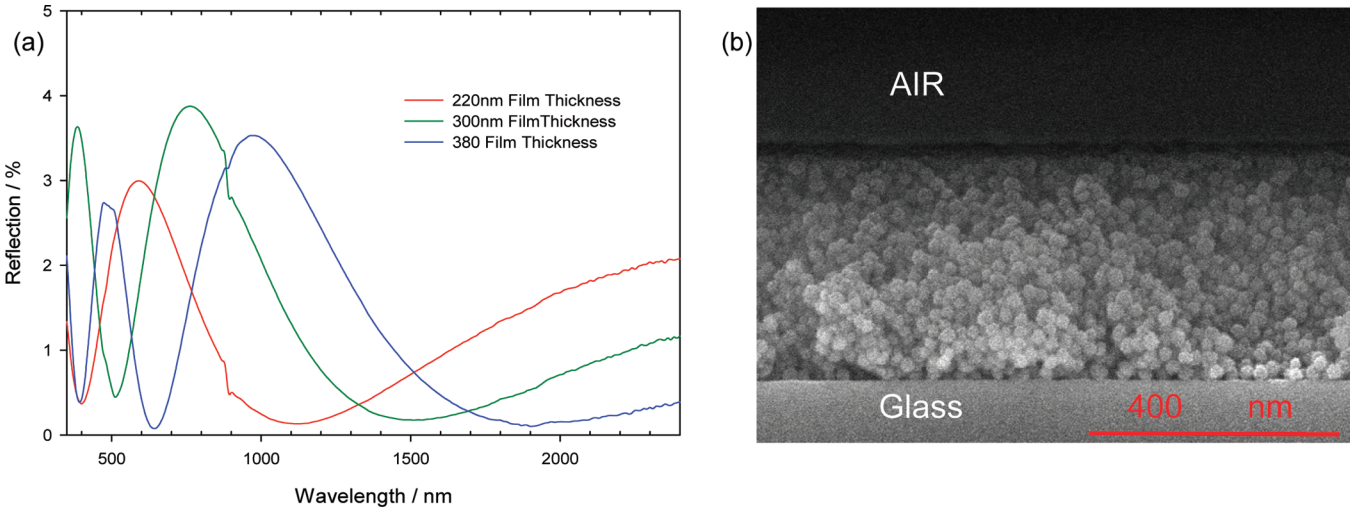

Figure 6. (a) Reflection spectra showing effect of increasing thickness variation of ARC thin films. (b) SEM image of ARC with reflection minimum at 1900 nm.

CONCLUSION

Single-layer antireflection coatings based on mesoporous silica nanoparticles have been demonstrated to be capable of reducing reflectance from a typical window surface to less than 0.1%. This is achieved by designing the layer such that the combination of nanoparticles and binders matches almost exactly the properties required for zero reflectance on glass, namely a refractive index of 1.28 and a film thickness of 120 nm. The ARC has a hardness of 4.4 GPa and passes a 5H pencil test. The thickness of the films can be varied and the reflection minimum can be tuned out as far as 1900 nm. These optical properties show significant improvement on those current available using vacuum and sol−gel single-layer techniques.

AUTHOR INFORMATION

Corresponding Author

*E-mail: jonathan.moghal@oxfordsurfaces.com.

ACKNOWLEDGMENTS

This Partnership received financial support from the Knowledge Transfer Partnerships programme (KTP). KTP aims to help businesses to improve their competitiveness and productivity through the better use of knowledge, technology and skills that reside within the UK Knowledge Base. KTP is funded by the Technology Strategy Board along with the other government funding organizations. The authors thank the CEMMNT network and BegbrokeNano for structural characterisation.

REFERENCES

(1) Cid, M.; Stem, N.; Brunetti, C.; Beloto, A. F.; Ramos, C. A. S. *Surf. Coat. Technol.* **1998**, *106*, 117−120.
(2) Lee, M.H..; Cho, J. S. *Thin Solid Films* **2000**, *365*, 5−6.
(3) Cannavale, A.; Fiorito, F.; Manca, M.; Tortorici, G.; Cingolani, R.; Gigli, G. *Building Environ.* **2010**, *45*, 1233−1243.
(4) Schulz, U.; Kaiser, N. *Prog. Surf. Sci.* **2006**, *81*, 387−401.
(5) Yoldas, B. E. *Appl. Opt.* **1980**, *19*, 1425−1433.
(6) Thomas, I. M. *Appl. Opt.* **1992**, *31*, 6145−6149.
(7) Ibn-Elhaj, M.; Schadt, M. *Nature* **2001**, *410*, 796−799.
(8) Prevo, B. G.; Hwang, Y.; Velev, O. D. *Chem. Mater.* **2005**, *17*, 3642−3651.
(9) Xi, J.-Q.; Kim, J. K.; Schubert, E. F. *Nano Lett.* **2005**, *5*, 1385−1387.
(10) Hecht, E. *Optics*, 4th ed.; Addison Wesley: Boston, MA, 2006; p 95.
(11) Knittl, Z. *Opt. Acta* **1978**, *25* (2), 167−173.
(12) Oyama, T.; Yamada, T. *Vacuum* **2000**, *59*, 479−483.
(13) Minemoto, T. A.; Takakura, H.; Hamakawa, Y. *Sol. Energy Mater. Sol. Cells* **2006**, *90*, 3576−3582.
(14) Dumas, L.; Quesnel, E. *J. Vac. Sci. Technol.* **2002**, *20*, 102−106.
(15) Kuo, M. L.; Poxson, D. J.; Kim, Y. S.; Mont, F. W.; Kim, J. K.; Schubert, E. F.; Lin, S. Y. *Opt. Lett.* **2008**, *33*, 2527−2529.
(16) Ganesha Shanbhogue, H.; Nagendra, C. L.; Annapurna, M. N.; Ajith Kumar, S.; Thutupalli, G. K. M. *Appl. Opt.* **1997**, *36*, 6339−6351.
(17) Dobrowolski, J. A.; Guo, Y.; Tiwald, T.; Ma, P. I.; Poitras, D. *Appl. Opt.* **2006**, *45*, 1555−1562.
(18) Lee, D.; Rubner, M. F.; Cohen, R. E. *Nano Lett.* **2006**, *10*, 2305−2312.
(19) Kuo, M. L.; Poxson, D. J.; Kim, Y. S.; Mont, F. W.; Kim, J. K.; Schubert, E. F.; Lin, S. Y. *Opt. Lett.* **2008**, *33*, 2527−2529.
(20) Mahdjoub, A.; Zighed, L. *Thin Solid Films* **2005**, *478*, 299−304.
(21) Thetford, A. *Opt. Acta* **1969**, *16*, 37−72.
(22) Lockhart, L. B.; King, P. J. *Opt. Soc. Am.* **1947**, *37*, 689.
(23) Schröder, D. *Phys. Thin Films* **1969**, *5*, 87.
(24) Dislich, H.; Hussmann, E. *Thin Solid Films* **1981**, *77*, 129−139.
(25) Prado, R.; Beobide, G.; Marcaide, A.; Goikoetxea, J.; Aranzabe, A. *Sol. Energy Mater. Sol.* **2010**, *94*, 1081−1088.
(26) San Vicente, G.; Baýon, R.; Gerḿan, N.; Morales, A. *Thin Solid Films* **2009**, *517*, 3157−3160.
(27) Fan, H. Y.; Wright, A.; Gabaldon, J.; Rodriguez, A.; Brinker, C. J.; Jiang, Y. B. *Adv. Funct. Mater.* **2006**, *16*, 891−895.
(28) Hoshikawa, Y.; Yabe, H.; Nomura, A.; Yamaki, T.; Shimojima, A.; Okubo, T. *Chem. Mater.* **2010**, *22*, 12−14.
(29) Nostell, P.; Roos, A.; Karlsson, B. *Thin Solid Films* **1999**, *351*, 170−175.
(30) Lien, S. Y.; Wuu, D. S.; Yeh, W. C.; Liu, J. C. *Sol. Energy Mater. Sol. Cells* **2006**, *90*, 2710−2719.
(31) Hammaberg, E.; Roos, A. *Thin Solid Films* **2000**, *442*, 222−226.
(32) Chabas, A.; Lombardo, T.; Cachier, H.; Pertuisot, M. H.; Oikonomou, K.; Falcone, R.; Verita, M.; Geotti-Bianchini, F. *Build. Environ.* **2008**, *43*, 2124−2131.
(33) Chen, D.; Yan, Y.; Westenberg, E.; Niebauer, D.; Sakaitani, N.; Chaudhuri, R. *J. Sol−Gel Sci. Technol.* **2000**, *19*, 77−82.
(34) Xiangmei, L.; Junhui, H. *J. Phys. Chem. C.* **2009**, *113*, 148−152.
(35) Zhao, Y.; Mao, G.; Wang, J. *Opt. Lett.* **2005**, *30*, 1885−1887.
(36) Nakajima, A.; Abe, K.; Hashimoto, K.; Watanabe, T. *Thin Solid Films* **2000**, *376*, 140−143.

(37) Du, Y.; Luna, L. E.; Tan, W. S.; Rubner, M. F.; Cohen, R. E. *ACS Nano* **2010**, *4*, 4308−4316.
(38) Du, X.; He, H. *Chem.—Eur. J.* **2011**, *17*, 8165−8174.
(39) Gemici, Z.; Shimomura, H.; Cohen, R. E.; Rubner, M. F. *Langmuir* **2008**, *24*, 2168−2177.
(40) *IUPAC Compendium of Chemical Technology*, 2nd ed.; McNaught, G. D., Wilkinson, A., Eds.;Blackwell Scientific Publications: Oxford, U.K., 1932; Vol *31*, p 577.
(41) Malzbender, J.; de With, G. *J. Non-Crystalline Solids* **2000**, *265*, 51−60.
(42) Luo, K.; Zhou, S.; Wu, L.; You, B. *Thin Solid Films* **2010**, *518*, 6804−6810.
(43) Camero, M.; Gordillo-Vázquez, F. J.; Gómez-Aleixandre, C. *Chem. Vap. Deposition.* **2007**, *13*, 326−334.
(44) Liu, B. T.; Ye, W. D.; Wang, W. H. *J. Appl. Polym. Sci.* **2010**, *118*, 1615−1619.
(45) Colts Standard Test L-11−12−05, "Steel Wool Abrasion" Colts Laboratories.
(46) Caro, J.; Cuadrado, N.; González, I.; Casellas, D.; Prado, J. M.; Vilajoana, A; Artús, P.; Peris, S.; Carrilero, A.; Dürsteler, J. C. *Surf. Coat. Technol.* **2011**, *205*, 5040−5052.
(47) Kobler, J.; Bein, T. *ACS Nano* **2008**, *2*, 2244−2330.